Journal of Structural Geology, Vol. 14, No. 4, pp. 475 to 489, 1992
Printed in Great Britain

0191-8141/92 $05.00+0.00

Structural and geochronologic relations along the western flank of the Coast Mountains batholith: Stikine River to Cape Fanshaw, central southeastern Alaska

W. C. McClelland,* G. E. Gehrels, S. D. Samson† and P. J. Patchett

Department of Geosciences, University of Arizona, Tucson, AZ 85721, U.S.A.

(*Received* 11 *March* 1991; *accepted in revised form* 14 *November* 1991)

Abstract—Geologic and U–Pb geochronologic studies in central southeastern Alaska provide constraints on the mid-Cretaceous to mid-Tertiary deformation west of the Coast Mountains batholith. The NE-dipping Sumdum and Fanshaw faults record the W-directed emplacement of the Ruth assemblage (Yukon–Tanana terrane) and Taku terrane over the subjacent Gravina belt and Alexander terrane. Ductile fabrics of the Sumdum–Fanshaw fault system truncate early-formed foliation and thrust faults in Albian and older Gravina belt strata. U–Pb age data from syn- and post-tectonic plutons suggest that deformation was ongoing at 92.9 ± 3.0 Ma but had mostly ceased by 90 Ma. The Sumdum–Fanshaw fault system marks the tectonic boundary between the Alexander–Wrangellia terrane and inboard Yukon–Tanana and Stikine terranes and lies within a thrust belt that extends from southern Alaska to northern Washington.

Mid-Cretaceous structures are truncated to the east by NE-dipping ductile fabrics of the Coast shear zone. Sheet-like Paleocene tonalites were emplaced into and deformed within the shear zone. Undeformed mid-Eocene dikes cross-cut the tonalites. Kinematic relations in the Coast shear zone suggest a complex displacement history that includes both east-side-up (reverse) and west-side-up (normal) shear. The shear zone probably accommodated the collapse of overthickened crust developed during mid-Cretaceous shortening.

INTRODUCTION

The Alexander–Wrangellia terrane has long been recognized as an allochthonous component of the western North American margin (e.g. Jones *et al.* 1972, 1977). In southeastern Alaska, the Alexander terrane is separated from the Stikine terrane to the east by metamorphic and plutonic rocks within and west of the Coast Mountains batholith (Fig. 1). Rocks west of the batholith record mid-Cretaceous shortening generally attributed to accretion of the Alexander–Wrangellia terrane (e.g. Monger *et al.* 1982, Coney & Jones 1985, Crawford *et al.* 1987). Alternatively, the Alexander terrane may have been accreted to the North American margin in mid-Jurassic time and mid-Cretaceous deformation served primarily to modify the earlier accretionary boundary (McClelland & Gehrels 1990, Saleeby & Rubin 1990, Rubin & Saleeby in press). Late Cretaceous and Tertiary structures, including the Coast Range megalineament (Twenhofel & Sainsbury 1958, Brew & Ford 1978), are superimposed on the mid-Cretaceous contractional belt and have apparently accommodated substantial uplift along the western margin of the batholith (e.g. Hollister 1982, Crawford *et al.* 1987). Mid-Cretaceous to Early Tertiary deformation was broadly coeval with and perhaps enhanced by (Hollister & Crawford 1986, Crawford & Crawford 1991) emplacement of arc-related calc-alkaline plutons within and west of the Coast Mountains batholith (Armstrong 1988, Arth *et al.* 1988, Barker & Arth 1990).

Metamorphic and plutonic rocks west of the Coast Mountains batholith provide an opportunity to examine the processes by which crustal fragments are added to continental margins. This paper outlines the mid-

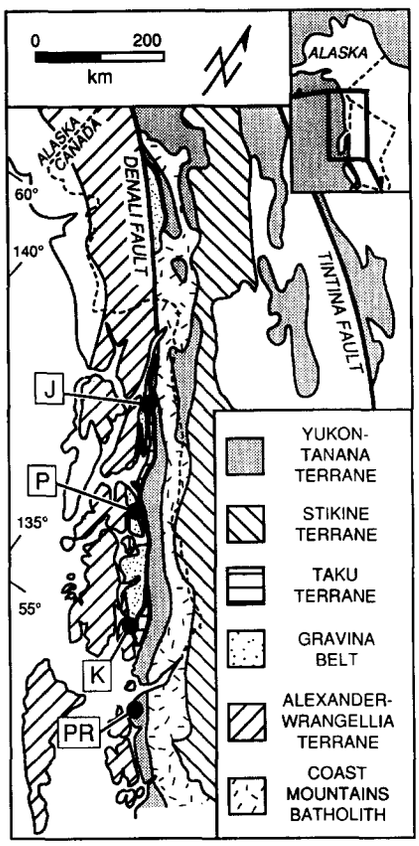

Fig. 1. Simplified terrane map of southeastern Alaska and northwestern Canada modified from Monger & Berg (1987) and Wheeler & McFeely (1987). Study area is located in the Petersburg (P) region. J = Juneau, K = Ketchikan and PR = Prince Rupert.

*Current address: Department of Geological Sciences, University of California, Santa Barbara, CA 93106, U.S.A.

†Current address: Department of Geology, Syracuse University, Syracuse, NY 13244-1077, U.S.A.

Cretaceous and Early Tertiary deformational history of rocks west of the Coast Mountains batholith in the Petersburg region, between Cape Fanshaw and the Stikine River (Figs. 1 and 2).

GEOLOGIC SETTING OF CENTRAL SOUTHEASTERN ALASKA

Kuiu and western Kupreanof Islands are underlain by low-grade Paleozoic and Upper Triassic rocks of the Alexander terrane (Fig. 2) (Berg *et al.* 1972, Brew *et al.* 1984). Deformed Alexander terrane strata in the mid-Jurassic Duncan Canal shear zone are unconformably overlain by tuffaceous turbiditic strata and mafic volcanic and volcaniclastic rocks of the Gravina belt (Berg *et al.* 1972, McClelland & Gehrels 1990). Gravina belt rocks, ranging from Oxfordian to Albian and possibly Cenomanian in age (Berg *et al.* 1972, Brew *et al.* 1984, Gehrels *et al.* in press), were most likely deposited in an intra-arc basinal setting (Berg *et al.* 1972, Rubin & Saleeby 1991b, McClelland *et al.* 1992).

The metamorphic grade and intensity of deformation within the Gravina belt rocks increases to the east where they are structurally overlain by upper greenschist to upper amphibolite facies metamorphic rocks. The overlying rocks include (1) a structurally lower sequence of metapelite, marble and minor metabasalt referred to as the Taku terrane, and (2) the Ruth assemblage: an eastern assemblage of metapelite, marble, quartzose metaclastic rocks, mafic metavolcanic rocks and mid-Paleozoic felsic metavolcanic rocks and granodioritic orthogneiss (Fig. 2) (McClelland *et al.* 1992). The Ruth assemblage and similar rocks exposed to the north (Port Houghton, Endicott Arm and Tracy Arm assemblages) are correlated with the Yukon–Tanana terrane (Gehrels *et al.* 1990, 1991a, in press, Samson *et al.* 1991, McClelland *et al.* 1992).

Rocks west of the Coast Mountains batholith are intruded by a mid-Cretaceous suite of gabbro, diorite, tonalite and granodiorite (Fig. 2) (Brew *et al.* 1984). The western margin of the Coast Mountains batholith is marked by a belt of elongate Late Cretaceous and Paleocene, tonalitic to granodioritic plutons (Fig. 2) that extends throughout southeastern Alaska (Brew & Ford 1981, Gehrels & Berg 1984, Gehrels *et al.* 1991b). Large

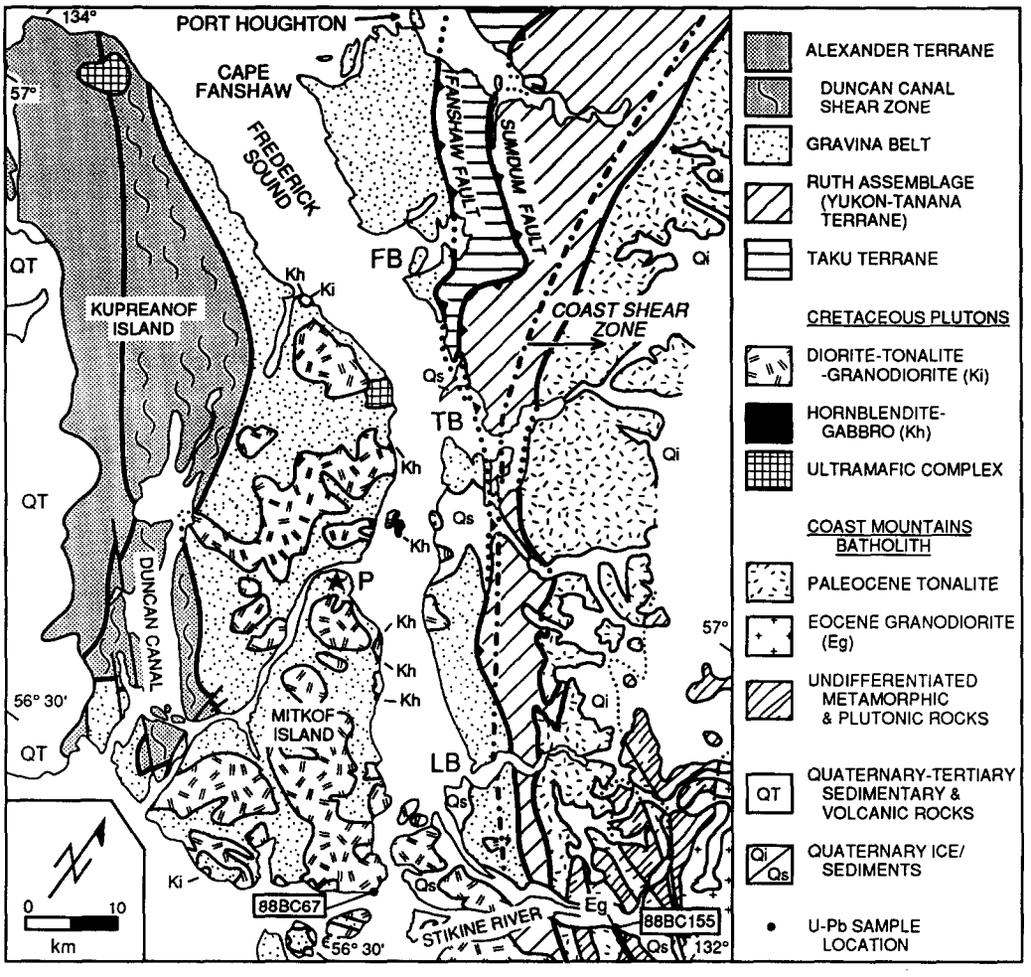

Fig. 2. Geologic map showing the location of major structural features in the Petersburg region, central southeastern Alaska. The western boundary of Coast shear zone is shown but the eastern boundary is not observed in the study area. Mapping during this study was generally restricted to shoreline traverses. Inland map relations are adapted from Buddington & Chapin (1929), Brew *et al.* (1984) and Gehrels & Berg (1984). LB = Le Conte Bay, TB = Thomas Bay, FB = Farragut Bay, P = Petersburg.

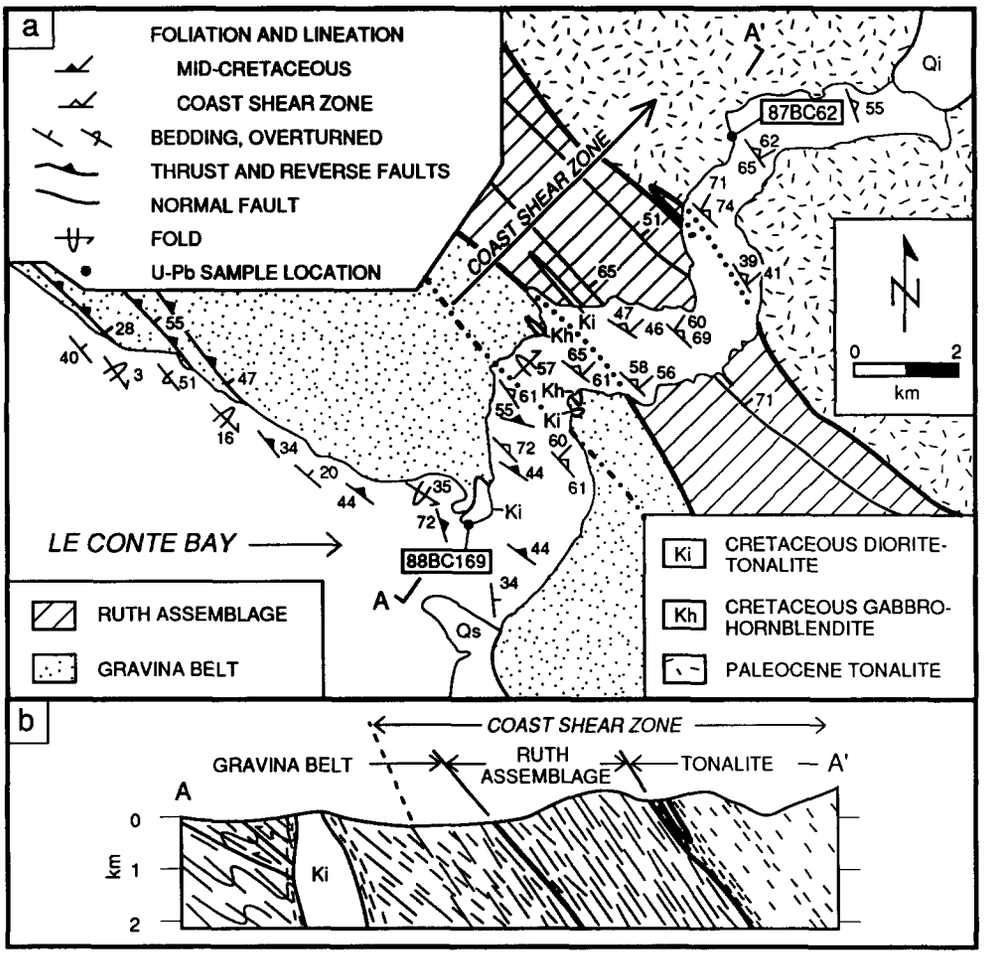

Fig. 3. Geologic map and schematic structural cross-section of Le Conte Bay (see Fig. 2 for location) showing U–Pb sample locations. Sample 88BC169 is located on Indian Point.

Eocene granodioritic plutons within the batholith form a third regional plutonic suite (Fig. 2) (Brew *et al.* 1984).

This article focuses on the age and character of mid-Cretaceous and younger structural elements that deform and separate the Gravina belt, Taku terrane and Ruth assemblage in the Petersburg region. McClelland *et al.* (1991, 1992) outlined thermobarometric results and the protolith character of the Gravina belt, Taku terrane and Ruth assemblage in this region.

GEOCHRONOLOGY

Samples for U–Pb (zircon) analysis were collected from the mid-Cretaceous, Paleocene and Eocene intrusive suites to constrain the age of deformation in the Petersburg region. Analytical procedures are described in Gehrels (1990).

Mid-Cretaceous plutons

Samples collected from the mid-Cretaceous suite include (1) lineated hornblende tonalite exposed at Blaquiere Point, southeastern Mitkof Island (Fig. 2), (2) granodiorite exposed on Indian Point at the mouth of Le Conte Bay (Fig. 3) and (3) tonalite in southern Thomas Bay (Fig. 4). The Blaquiere Point and Indian Point samples yielded discordant analyses (Fig. 5 and Table 1). Fractions from the Blaquiere Point sample define a chord with intercepts of 92.9 ± 3.0 and 970 ± 380 Ma (Fig. 5a). Fractions from the pluton on Indian Point define a similar chord with intercepts of 91.3 ± 6.3 Ma and 940 ± 290 Ma (Fig. 5b). The plutons intrude Upper Jurassic–Lower Cretaceous Gravina belt strata so the lower intercept must indicate the crystallization age. This is consistent with the clustering of fractions from both samples near the lower intercept, the expected pattern of magmatic zircons that contain slight components of inherited zircon. The upper intercept ages suggest a Late Proterozoic age for the average inherited component. This inheritance may reflect magmatic interaction with the Alexander terrane basement or incorporation of Proterozoic zircons from the Gravina belt. In addition, the upper intercept ages are similar to the age of detrital zircons analyzed from the Port Houghton assemblage (Gehrels *et al.* 1991a) suggesting that metamorphic rocks structurally above the Gravina belt to the east may also stratigraphically or structurally underlie the Gravina belt.

Zircon fractions analyzed from a strongly deformed tonalitic orthogneiss that roughly parallels foliation in the adjacent Ruth assemblage in southern Thomas Bay

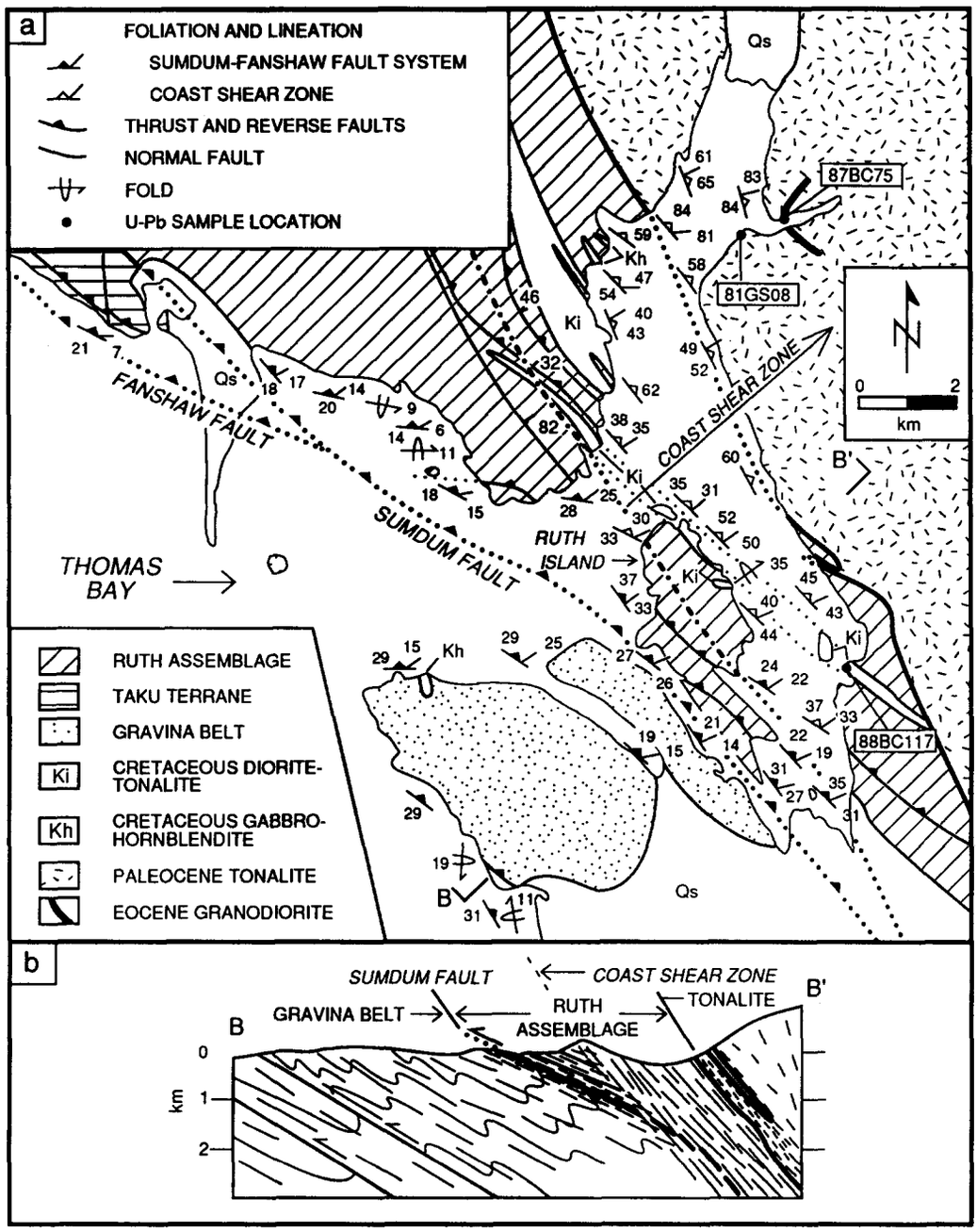

Fig. 4. Geologic map and schematic structural cross-section of Thomas Bay (see Fig. 2 for location) showing U–Pb sample localities.

(Fig. 4) overlap (at the 95% confidence level) but are spread along concordia (Fig. 5c and Table 1). The degree of discordance varies with zircon size and U concentration and an abraded fraction yielded nearly concordant results. These relations and the observation that the sample was deformed at temperatures exceeding 600°C during Paleocene time (McClelland *et al.* 1991) suggest that the discordance is likely due to Pb loss. Accordingly, an emplacement age of 99 ± 5 Ma is inferred for the pluton.

Paleocene plutons

Samples for U–Pb analysis were collected from weakly foliated, homogenous portions of tonalite plutons in Le Conte Bay (Fig. 3) and Thomas Bay (Fig. 4). Concordant analyses from both samples indicate an emplacement age of 59.5 ± 1.0 Ma for the tonalite in Le Conte Bay (Fig. 6a and Table 1) and 63.5 ± 1.0 Ma for the tonalite in Thomas Bay (Fig. 6b and Table 1). The latter determination revises a previously reported preliminary age of 64 ± 2 Ma obtained from the Thomas Bay sample (Gehrels *et al.* 1984). These ages are consistent with reported U–Pb ages of 83–57 Ma from similar tonalites along the western margin of the Coast Mountains batholith from Skagway to Prince Rupert (Gehrels *et al.* 1991b).

Eocene dikes

Samples of W-dipping leucocratic granodiorite dikes from Thomas Bay (Fig. 4) and along the Stikine River

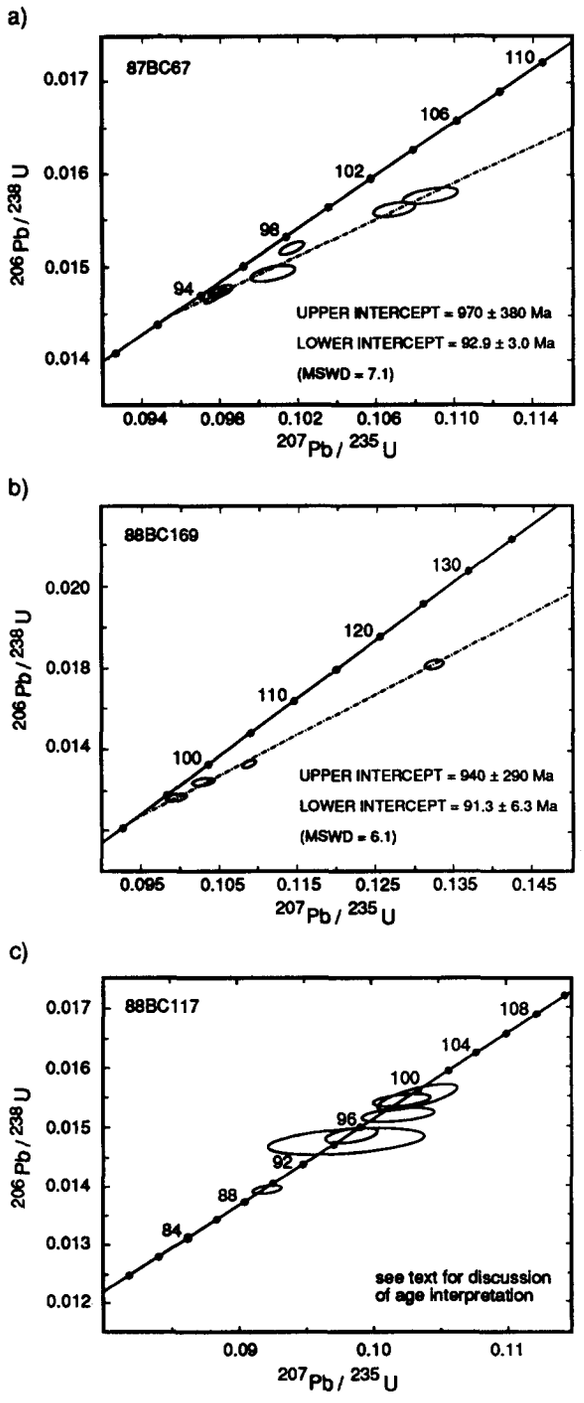

Fig. 5. U–Pb concordia plots of zircon fractions from mid-Cretaceous plutonic rocks (Table 1): (a) tonalite on Blaquiere Point (Fig. 2); (b) granodiorite at Indian Point (Fig. 3); and (c) tonalite in southern Thomas Bay (Fig. 4).

(Fig. 2) yielded discordant results. Fractions from the Thomas Bay dike define a line with intercepts of 50 ± 6.5 Ma and 300 ± 120 Ma (Fig. 7a and Table 1). The lower intercept is interpreted as the emplacement age since the dike intrudes Paleocene tonalite and the discordance likely reflects an inherited zircon component. Dispersion in the data is inferred to reflect heterogeneity in the age of the inherited components. Although a meaningful emplacement age cannot be determined from analyses of the Stikine River sample (Fig. 7b and Table 1), the zircon systematics are similar to those of the Thomas Bay dike and an emplacement age of approximately 50 Ma is inferred by comparison with the age determination in Thomas Bay. The dike emplacement ages are consistent with K–Ar cooling ages of 51.3 ± 1.5 Ma (biotite) and 49.3 ± 1.5 Ma (hornblende) obtained from a compositionally similar Eocene granodiorite east of Le Conte Bay (Fig. 2) (Brew *et al.* 1984, Douglass *et al.* 1989).

STRUCTURAL GEOLOGY

Mid-Cretaceous deformation

The Gravina belt, Taku terrane and Ruth assemblage are separated by the mid-Cretaceous Sumdum and Fanshaw faults (Figs. 1 and 2) (Gehrels *et al.* 1990, in press). These structures lie within a 5–20-km-wide W-vergent fault system, informally called the Sumdum–Fanshaw fault system. Additional mid-Cretaceous structural elements include early-formed regional fabrics in the Gravina belt and fabrics related to emplacement of undeformed mid-Cretaceous plutons (Fig. 8).

Early-formed fabrics in the Gravina belt include NE-dipping thrust faults, regional foliation and folds. The Alexander terrane and westernmost Gravina belt on Kupreanof Island are cut by a poorly- to moderately-developed spaced cleavage. To the east on Mitkof and northeastern Kupreanof Islands (Fig. 8), the Gravina rocks possess a moderately- to well-developed foliation defined by alignment of micaceous minerals and flattening fabrics. Regionally, the foliation strikes northwest and dips moderately northeast but attitudes are locally variable due to disruption during pluton emplacement (Fig. 8). The regional foliation is axial planar to abundant open to tight upright folds that typically plunge 5–30° to the east-southeast. Asymmetric folds are overturned to the southwest.

Shallowly to moderately NE-dipping, sub-km-spaced thrust faults that imbricate the Gravina belt are best exposed on southern Mitkof Island. The faults, recognized as 0.5–2-m-thick, phyllonitic zones, often parallel compositional layering and regional foliation in the hanging wall strata but truncate strongly folded fabrics in footwall rocks. Asymmetric folds adjacent to the faults are SW-vergent, indicating SW-directed transport. Meter-scale, top-to-the-southwest offsets are observed on smaller faults. Magnitude of displacement on larger faults is uncertain. The thrust faults are inferred to be kinematically linked with the regional foliation and W-vergent folds in the Gravina belt.

Early-formed cleavage in Gravina strata on Cape Fanshaw define a km-scale E-plunging antiform (Fig. 8). In western Farragut Bay, the strike of the cleavage rotates to a more northerly trend, reflecting the large-scale folding (Figs. 9 and 10c). The fold post-dates the regional Gravina foliation but is truncated by the Sumdum–Fanshaw fault system.

Approaching the Fanshaw fault in Farragut Bay (Fig.

Table 1. U–Pb isotopic data and apparent ages

Size (μm)	Weight (mg)	Concentration (ppm) U	Pb*	Isotopic composition $\frac{^{206}Pb}{^{204}Pb}$	$\frac{^{206}Pb}{^{207}Pb}$	$\frac{^{206}Pb}{^{208}Pb}$	Apparent ages (Ma) $\frac{^{206}Pb^*}{^{238}U}$	$\frac{^{207}Pb^*}{^{235}U}$	$\frac{^{207}Pb^*}{^{206}Pb^*}$
87BC67—tonalite on Blaquiere Point (132°32′33″, 56°35′07″)									
0–45	6.40	972.1	13.732	4484(210)	19.452(10)	13.390(8)	94.3(0.3)	94.9 (0.5)	109(12)
30–45	1.79	1054.7	14.808	8540(100)	20.029(24)	14.558(39)	93.9(0.3)	94.6 (0.4)	113(9)
100–125	24.76	810.2	11.510	4166(420)	19.100(38)	14.900(30)	95.5(0.4)	97.4 (0.9)	143(20)
100–125[a]	1.11	560.7	8.570	740(6)	14.350(50)	7.813(17)	100.7(0.05)	104.76(1.1)	197(23)
125–145[a]	3.59	556.5	8.367	1620(30)	17.052(75)	10.682(36)	99.8(0.4)	103.1 (0.9)	180(11)
145–175	6.90	415.8	6.090	2850(80)	18.660(20)	11.732(2)	97.2(0.4)	98.3 (0.5)	125(12)
88BC169—granodiorite on Indian Point (132°31′29″, 56°44′57″)									
30–45	1.78	950.2	12.967	614(1)	13.800(12)	11.888(9)	94.9(0.5)	96.3 (1.1)	132(22)
45–63	1.64	825.2	11.584	630(7)	13.840(19)	11.795(14)	97.3(0.5)	99.5 (1.2)	151(26)
63–80	2.06	787.0	11.410	1295(4)	16.230(18)	17.330(40)	100.0(0.4)	104.8 (0.6)	215(13)
100–175	1.16	556.9	9.628	946(9)	14.646(16)	10.410(7)	115.7(0.5)	126.2 (1.0)	329(16)
88BC117—tonalite in southern Thomas Bay (132°47′05″, 56°59′35″)									
30–45	2.88	369.6	5.166	1360(20)	17.05 (10)	6.962(21)	89.3(0.3)	89.6 (0.9)	98(23)
80–100	2.06	322.7	4.957	194(2)	8.050(80)	2.930(18)	94.4(1.2)	95.0 (4.6)	111(103)
100–125	2.76	285.9	5.420	408(2)	11.906(18)	4.030(7)	95.0(0.6)	95.4(1.6)	104(34)
125–145	2.14	298.9	4.855	298(1)	10.255(16)	3.486(2)	99.2(1.1)	100.0 (2.4)	119(40)
145–175	2.51	292.6	4.660	384(2)	11.540(80)	3.850(10)	97.3(0.6)	98.6 (2.2)	131(47)
145–175[a]	3.35	294.4	4.804	652(10)	14.20 (10)	4.300(5)	98.8(0.5)	98.8 (1.7)	99(37)
87BC62—tonalite in Le Conte Bay (132°26′26″, 56°48′58″)									
80–100	2.95	470.8	4.374	544(5)	13.500(67)	5.576(10)	59.7(0.3)	59.7 (1.0)	60(35)
100–125	3.70	362.6	3.341	813(10)	15.301(8)	6.548(1)	59.5(0.2)	59.7 (0.6)	68(21)
125–145	12.80	255.4	2.356	1115(30)	16.586(22)	7.205(6)	59.6(0.2)	59.6 (0.6)	59(23)
145–175	3.48	444.5	4.118	1030(5)	16.290(26)	6.944(10)	59.8(0.2)	59.8 (0.4)	59(2)
145–175	3.20	443.3	4.101	615(8)	14.100(49)	6.047(10)	59.8(0.3)	59.8 (0.9)	58(31)
81GS08—tonalite in Thomas Bay (132°49′12″, 57°04′29″)									
45–63	4.20	595.6	5.955	2690(40)	18.962(9)	6.615(2)	62.9(0.2)	63.0 (0.3)	68(11)
80–100	3.33	518.9	5.192	1880(30)	18.160(14)	6.720(3)	63.4(0.2)	63.4 (0.4)	66(13)
100–125	3.04	499.9	4.991	850(10)	15.485(15)	5.905(5)	63.4(0.3)	63.6 (0.6)	71(21)
125–145	3.91	431.4	4.315	598(4)	13.930(13)	5.418(2)	63.6(0.3)	63.7 (0.8)	65(26)
145–165	1.94	422.3	4.212	642(4)	14.250(16)	5.597(5)	63.6(0.3)	63.7 (0.7)	69(23)
87BC75—granodiorite dike in Thomas Bay (132°48′21″, 57°04′40″)									
20–30	0.48	1915.8	17.178	1158(10)	16.554(20)	5.621(11)	55.5(0.2)	56.3 (0.4)	90(15)
30–45	3.50	1424.0	12.571	2246(16)	18.490(15)	7.464(2)	56.5(0.2)	57.1 (0.3)	82(11)
45–63	13.80	1140.2	10.079	2300(58)	18.455(15)	8.079(6)	57.1(0.4)	57.9 (0.5)	93(13)
100–125	8.21	738.3	6.566	2127(43)	18.214(9)	8.775(5)	58.0(0.2)	59.0 (0.3)	103(12)
100–125[am]	2.43	615.2	5.870	3620(40)	19.275(10)	8.545(11)	61.6(0.2)	62.4 (0.3)	94(9)
125–145	9.45	623.3	5.423	1195(20)	16.685(15)	8.220(2)	57.0(0.2)	57.7 (0.5)	86(17)
145–175	9.15	531.8	4.628	1718(21)	17.800(9)	8.995(7)	57.1(0.2)	57.7 (0.3)	85(12)
100–175[a]	1.12	555.0	5.682	700(6)	14.405(58)	6.018(18)	65.6(0.3)	67.4 (0.8)	130(26)
88BC155—granodiorite dike along the Stikine River (132°09′30″, 56°42′02″)									
30–45	1.47	2096.3	18.515	457(4)	12.590(19)	4.470(2)	55.2(0.4)	55.5 (0.9)	68(35)
45–63	1.89	1677.5	14.435	1612(4)	17.775(14)	5.874(1)	53.7(0.2)	53.8 (0.3)	60(12)
63–80	3.24	1520.9	13.140	2589(28)	18.915(15)	6.522(5)	54.3(0.2)	54.5 (0.3)	64(11)
100–125	1.26	1223.9	10.808	436(3)	12.360(40)	4.894(4)	56.3(0.3)	56.6 (1.0)	69(37)
100–175[m]	0.65	1652.1	15.321	492(12)	12.890(61)	3.874(12)	56.0(0.3)	56.8 (1.3)	95(49)

*Radiogenic Pb.

[a]Abraded to 50–75% of original size.

[m]Magnetic fraction. All other fractions are non-magnetic at 1.7–1.8 A, 1–10° (side slope) and 10–20° (front slope) on Frantz magnetic separator.

Note: Analytical techniques are described in Gehrels (1990). Constants used: $\lambda^{238}U = 1.55125 \times 10^{-10}$; $\lambda^{235}U = 9.8485 \times 10^{-10}$; $^{238}U/^{235}U = 137.88$. Uncertainties (in parentheses) are reported at the 95% level. Isotopic compositions listed above have not been adjusted. In calculating concentrations and apparent dates, the measured isotopic ratios are adjusted for: (1) mass-dependent correction factors of 0.14% ± 0.1%/AMU for Pb, 0.11% ± 0.12% for U, and 0.24% ± 0.11% for UO_2; (2) 0.05 ± 0.025 to 0.02 ± 0.01 ng of blank Pb with isotopic composition $^{206}Pb/^{204}Pb = 18.6 \pm 0.3$, $^{207}Pb/^{204}Pb = 15.5 \pm 0.3$, and $^{208}Pb/^{204}Pb = 38.0 \pm 0.8$; and (3) 0.005 ± 0.003 to 0.0005 ± 0.0003 ng of blank U. Common Pb remaining after correcting for blank Pb is inferred to be initial Pb with a composition of $^{206}Pb/^{204}Pb = 18.5 \pm 2.0$, $^{207}Pb/^{204}Pb = 15.618 \pm 0.3$, and $^{208}Pb/^{204}Pb = 38.5 \pm 2.0$, approximated from Stacey & Kramers (1975).

Description of zircon populations: 87BC67: euhedral (Eu)-minor subhedral (Sb), 5–3:1 (aspect ratio, length:width), clear to pink, clear inclusions common. 88BC169: Eu, 2–4:1, clear to pink tint, clear inclusions common. 88BC117: anhedral, 1:2, clear colorless. 87BC62: Eu, 4–2:1, clear to pink tint. 81GS08: Eu–Sb, 2:1, clear with abundant dark inclusions. 87BC75: Eu, 3–2:1 and 5:1 rods, clear to pink tint, abundant clear inclusions and a few visible cores. 88BC155: Eu, 5–2:1, clear with abundant clear inclusions.

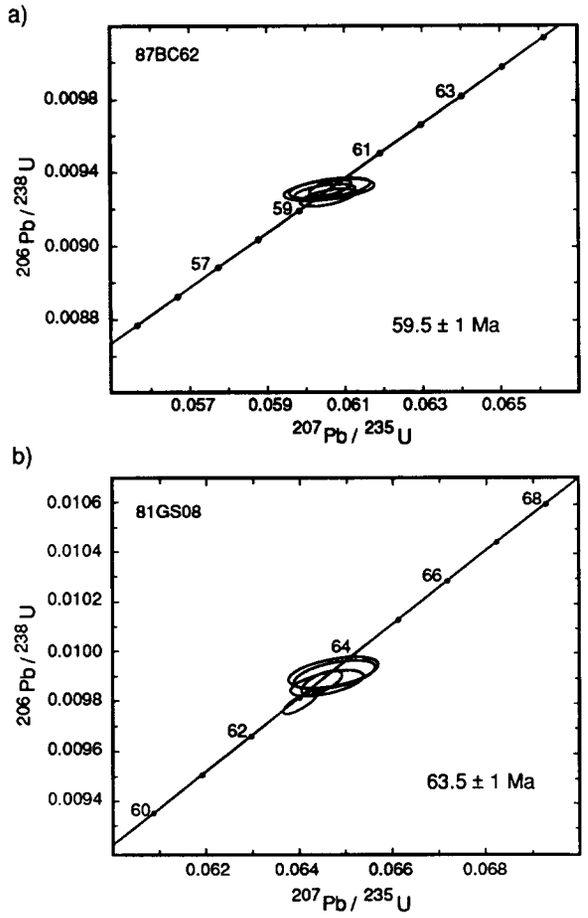

Fig. 6. U–Pb concordia plots of zircon fractions from Paleocene tonalites: (a) Le Conte Bay (Fig. 3); and (b) Thomas Bay (Fig. 4).

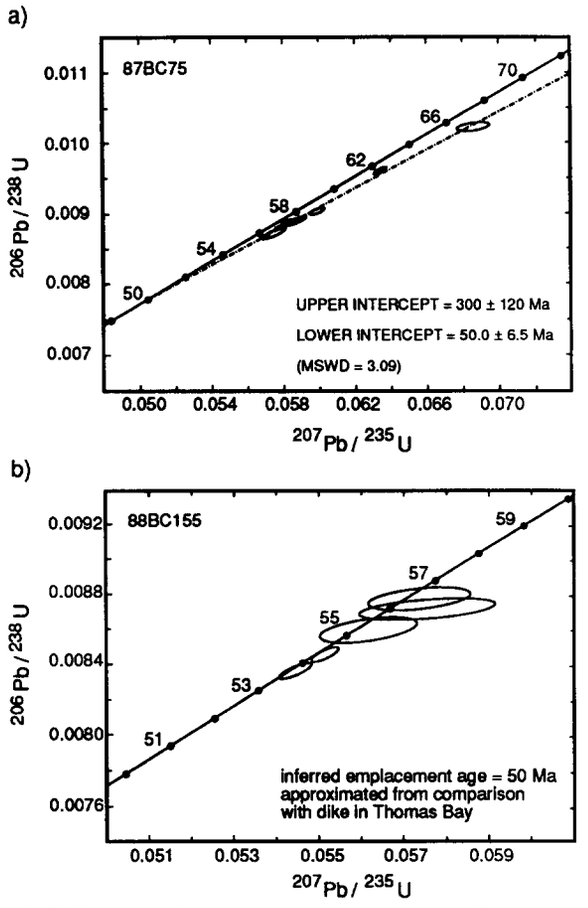

Fig. 7. U–Pb concordia plots of zircon fractions from Eocene granodiorite dikes exposed (a) in Thomas Bay (Fig. 4) and (b) along the Stikine River (Fig. 2).

9), early-formed fabrics are crenulated, truncated and rotated by a moderately (45–65°) NE-dipping spaced cleavage (Figs. 10d & e). Tight to isoclinal, upright to overturned (to the southwest) folds of the early cleavage and compositional layering plunge gently to the southeast in western exposures. Hinges of comparable folds in eastern exposures have a steeper, more easterly plunge and are colinear with down-dip mineral, elongation and cleavage intersection lineations (Figs. 10d & e). At structurally higher levels, rocks possess a penetrative NE-dipping foliation that is subparallel to SW-vergent thrust faults. Similar relations are observed below the Fanshaw fault in Port Houghton (Gehrels *et al.* in press) and Sumdum fault near Thomas and Le Conte Bays (Figs. 8 and 11c).

Within and southeast of Farragut Bay, the Fanshaw fault is a ductile shear zone that separates the Gravina belt and Taku terrane. The shear zone and foliation in the adjacent rocks dip 55–75° NE at the head of Farragut Bay and 20–40°NE on Frederick Sound (Fig. 10f). In Thomas Bay, the contact between the Gravina belt and Ruth assemblage lies within the channel west of Ruth Island (Fig. 4). Rocks along the channel possess a penetrative foliation, pronounced flattening fabrics, and significantly reduced grain size from that observed in rocks west and east of the channel. Hinges of mesoscopic isoclinal folds are colinear to down-dip stretching and mineral lineations (Figs. 11b & c). The Gravina belt–Ruth assemblage contact is interpreted as the Sumdum fault since it places higher-grade mid-Paleozoic rocks over lower-grade and younger Gravina belt rocks.

Rocks above the Sumdum fault are strongly folded and imbricated by NE-dipping shear zones, recognized as 1–3-m-thick zones of intense ductile, locally mylonitic, shearing that offset or truncate compositional layering and fold limbs. Penetrative foliation and transposed compositional layering are coplanar with the shear zones. Layer-parallel shears, recognized only where they locally cross-cut compositional layering, are also common. Tight to isoclinal folds with strongly sheared limbs and wavelengths of a few cm to over 10 m, plunge 15–30° to the east (Fig. 11c). Down-dip mineral and stretching lineations are parallel to those observed below the Sumdum fault. The above structures are interpreted to be kinematically linked and contemporaneous with the Sumdum fault.

Asymmetric folds with subhorizontal hinges adjacent to the Sumdum, Fanshaw and related faults are typically overturned to the southwest. Offsets across ductile shears and minor slip surfaces are SW-directed. Thin section-scale kinematic indicators, including *S–C* fabrics, shear bands, rotated porphyroclasts, and sigmoidal shape and displacement sense of deformed minerals, also indicate SW-directed transport of the Ruth assem-

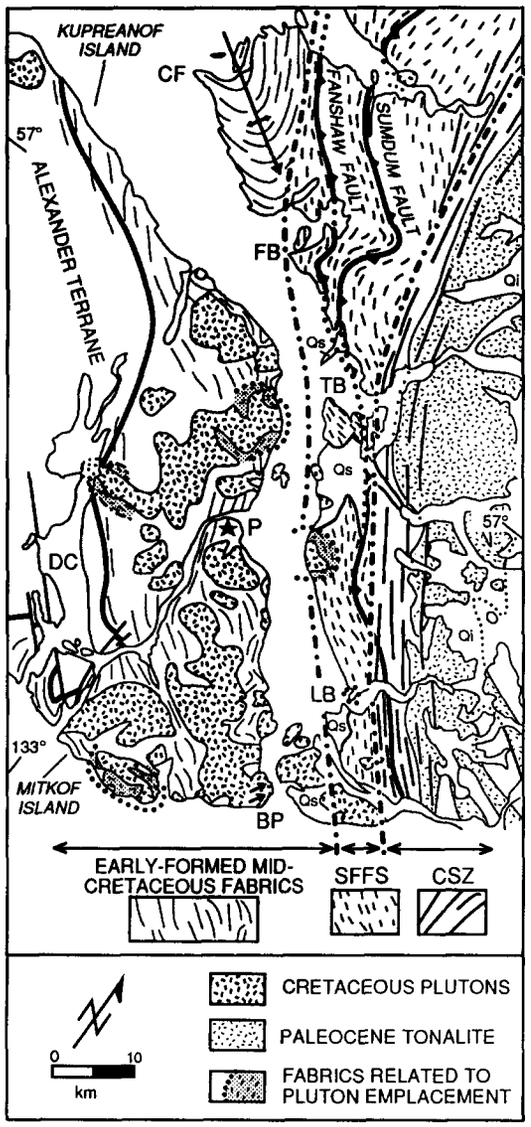

Fig. 8. Sketch map outlining the regional variation in the strike of: (1) early-formed mid-Cretaceous foliation; (2) foliation in the Sumdum–Fanshaw fault system (SFFS); and (3) Late Cretaceous to Paleocene Coast shear zone (CSZ) foliation. Arrows in pluton on Blaquiere Point (BP) show trend of moderately plunging lineation discussed in text. CF = Cape Fanshaw, FB = Farragut Bay, TB = Thomas Bay, LB = Le Conte Bay, DC = Duncan Canal.

blage. The transport direction is assumed to be parallel to the down-dip lineations which typically trend N60°–75°E (Figs. 10–12).

Age constraints on mid-Cretaceous deformation

The Sumdum–Fanshaw fault system and deformation of the Gravina belt are younger than the age of the youngest Gravina strata, i.e. Albian and possibly Cenomanian in age (Brew *et al.* 1984, Gehrels *et al.* in press). In addition, several observations suggest syn- and possibly pre-tectonic emplacement of several mid-Cretaceous plutons. First, weakly- to well-developed foliation in dikes that emanate from these plutons is coplanar to the wall rock foliation. Second, complex temporal relations exist between deformation and pluton emplacement on southern Mitkof Island where a non-foliated tonalite dike cross-cuts an E-dipping fault in the Gravina strata but is itself cut by a similar fault. Finally, the tonalite at Blaquiere Point (Fig. 8) contains a lineation, defined by the alignment of magmatic hornblende and mafic inclusions, that we infer formed as the pluton crystallized. This fabric is subparallel to mineral lineations in the wall rocks that formed during regional deformation. From these relations, we conclude that deformation resulting in the early-formed mid-Cretaceous fabrics was ongoing at 92.9 ± 3.0 Ma.

Undeformed mid-Cretaceous plutons cross-cut the regional foliation and locally impart a younger penetrative fabric to the wall rocks. As an example, bedding and early structures in Gravina strata adjacent to a pluton exposed on the eastern shore of Kupreanof Island, approximately 10 km north of Petersburg (Fig. 8), are isoclinally folded and cut by a well-developed axial planar foliation that parallels the pluton margin. The intensity of this fabric decreases away from the contact, grading into open to tight upright folds associated with a spaced axial-planar cleavage. K–Ar ages of 89.4 ± 2.7 Ma (hornblende) and 91.0 ± 2.7 Ma (biotite) determined for this pluton (Douglass *et al.* 1989) suggest that regional fabrics in this portion of the Gravina belt formed prior to approximately 90 Ma. Structures within the Sumdum–Fanshaw fault system are rotated and steepened adjacent to the unfoliated pluton at Indian Point (Figs. 3 and 12c). In addition, unfoliated dikes related to the pluton cross-cut wall rock fabrics. These relations suggest that ductile deformation in the Sumdum–Fanshaw fault system ceased prior to 91.3 ± 6.3 Ma. In Port Houghton, an undeformed pluton that apparently cross-cuts the Sumdum fault yields an emplacement age of 78 ± 8 Ma (Gehrels *et al.* in press), thus providing a minimum age for the Sumdum fault itself.

Based on the above age constraints, most mid-Cretaceous structures in the Gravina belt can be bracketed between Albian, ranging from 113 to 97.5 Ma (Palmer 1983), and approximately 90 Ma. This age range is similar to age constraints on deformation in the Ketchikan region (Rubin & Saleeby in press). The Sumdum–Fanshaw fault system and regional structures in the Gravina belt most likely evolved progressively, but the detailed history of strain partitioning across the belt has not been established. Hence, although it is our bias that the Sumdum–Fanshaw fault system is younger than the regional fabrics in the Gravina belt, it is uncertain to what extent the regional structures are actually contemporaneous with the Sumdum–Fanshaw fault system. Similarly, while most of the regional deformation apparently occurred prior to 90 Ma, partitioning of deformation to younger ductile structures in the Ruth assemblage cannot be precluded.

The foliation in the Ruth assemblage rocks is a penetrative composite fabric that evolved through transposition of previous planar fabrics. The composite fabric may be entirely mid-Cretaceous in age, recording mid-Cretaceous transposition cycles as described by Tobisch & Patterson (1987). More likely, the fabric is in part pre-

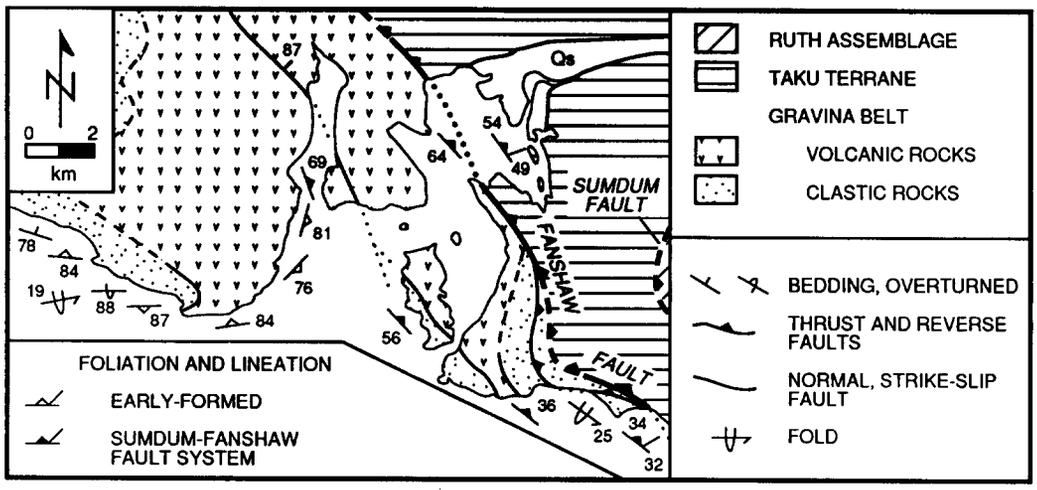

Fig. 9. Geologic map of Farragut Bay (see Fig. 2 for location).

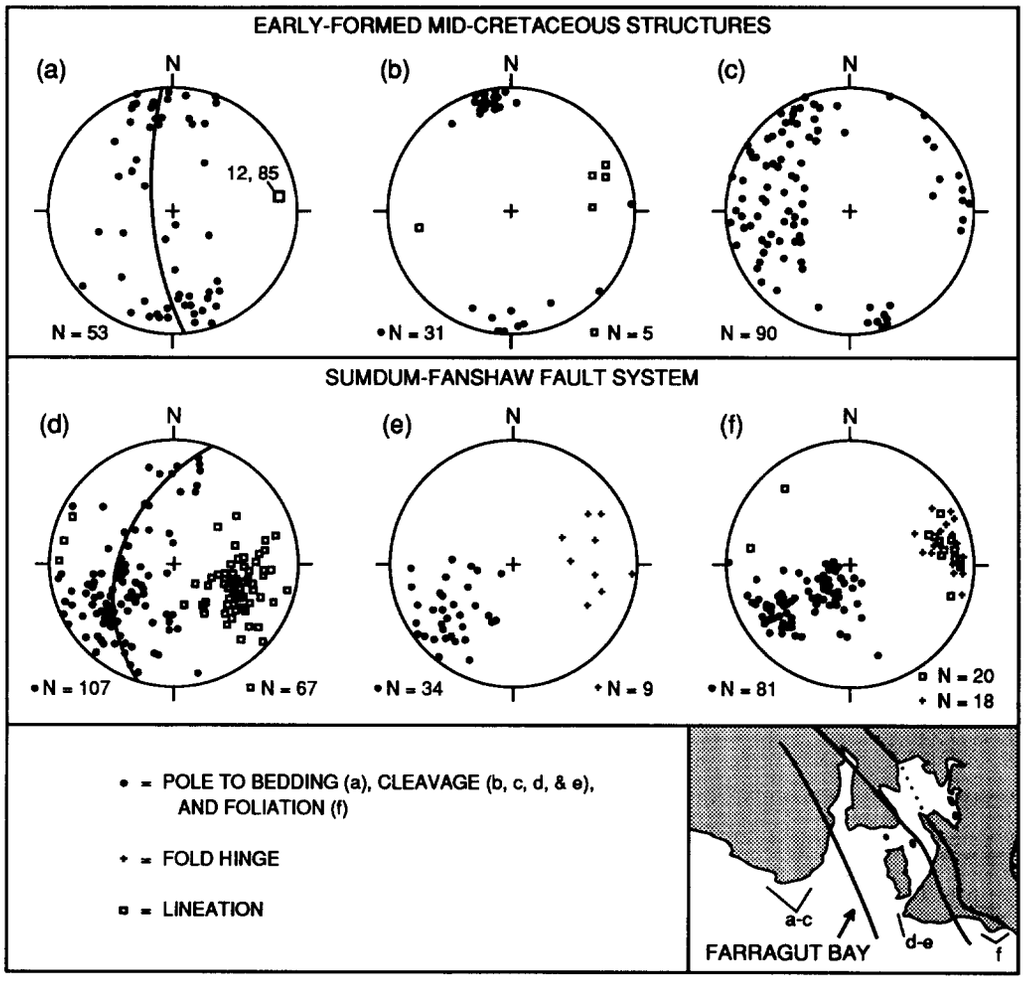

Fig. 10. Equal-area plots summarizing structural data from Farragut Bay (Fig. 9). Inset map outlines stereonet domains. Structural data in Figs. 10–12 were plotted and vector mean values determined using Stereonet (v.3.66) by R. W. Allmendinger. (a) Bedding attitudes on Cape Fanshaw. The pole distribution suggests folding about an axis of 12°, 85°. (b) Axial-planar cleavage and fold hinges west of Farragut Bay. (c) Cleavage along the western shore of Farragut Bay. (d) Early-formed cleavage and small-scale folds of this cleavage in the western SFFS. Poles to early-formed cleavage define great circle girdle with a pole of 34°, 108°. (e) Cleavage and intersection and mineral lineations in the western SFFS. Cleavage is axial planar to folds plotted in (d). (f) Foliation, fold hinges, and mineral and stretching lineations associated with the Fanshaw fault.

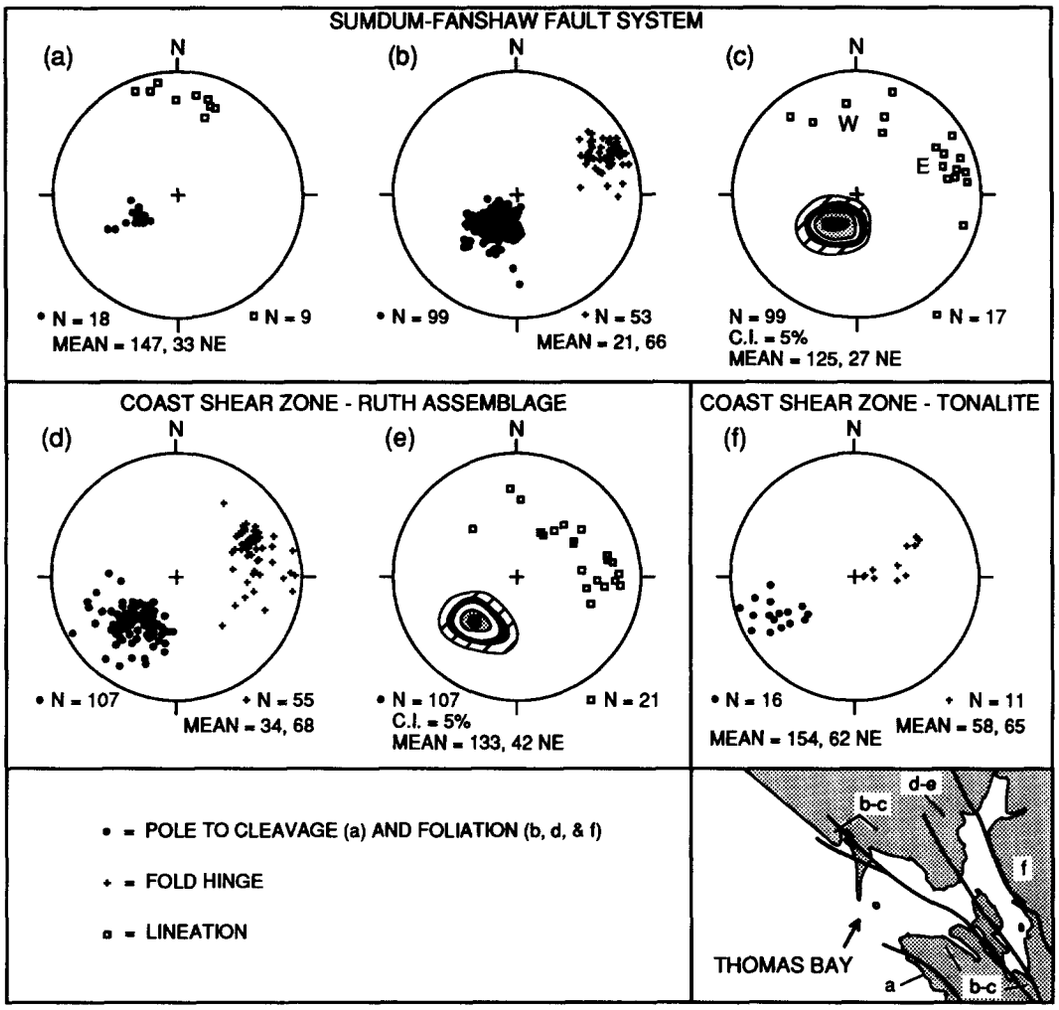

Fig. 11. Equal-area plots summarizing structural data from Thomas Bay (Fig. 4). Inset map outlines stereonet domains. (a) Cleavage and fold hinges in the westernmost SFFS. (b) Foliation and mineral stretching lineations associated with the Sumdum fault. (c) Fold hinges and contoured plot of foliation plotted in (b). Scatter reflects west (W) to east (E) rotation of fold hinges from a subhorizontal to down-dip plunge. (d) Coast shear zone (CSZ) foliation and mineral stretching lineations in the Ruth assemblage. (e) Fold hinges in the CSZ and contoured plot of foliation plotted in (d). (f) CSZ foliation and mineral lineation observed in the tonalite in Thomas Bay.

mid-Cretaceous in age, with older fabrics recording deformation and metamorphism yet to be resolved. Evidence for earlier metamorphism of the Yukon–Tanana terrane within the Coast Mountains is discussed by Gehrels *et al.* (1991a).

Late Cretaceous and Early Tertiary deformation

In Thomas and Le Conte Bays, a complex zone of steeply NE-dipping ductile fabrics, herein referred to as the Coast shear zone (previously Le Conte Bay shear zone of McClelland *et al.* 1991), deforms the Ruth assemblage and Paleocene tonalites and truncates mid-Cretaceous structural trends. This zone is roughly coincident with the Coast Range megalineament (Twenhofel & Sainsbury 1958, Brew & Ford 1978). In western Le Conte Bay, mid-Cretaceous layer-parallel foliation is progressively truncated, folded and transposed by the more steeply dipping Coast shear zone foliation (Fig. 3). Attitudes of the two foliations observed at single localities across the transition from mid-Cretaceous to Coast shear zone fabrics are slightly but significantly different (Fig. 12f). Mid-Cretaceous fabrics in Thomas Bay are cut by the steeper Coast shear zone foliation as well (Figs. 4 and 11c & e).

Metamorphic rocks in the Coast shear zone possess a moderately to steeply NE-dipping (Figs. 11d and 12g) foliation, defined by alignment of micaceous minerals, amphibole, and quartz ribbons, that is coplanar with compositional layering and transposed mid-Cretaceous foliation. These penetratively foliated blastomylonitic rocks are cut by 5- to 50-m-wide ductile shear zones. Hinges of isoclinal folds defined by compositional layering are colinear with down-dip stretching lineations (Figs. 11d & e and 12g & h). Small-scale folds are commonly asymmetric but there is no apparent preference in dextral vs sinistral vergence. Paleocene tonalites in Thomas Bay and Le Conte Bay possess a moderately- to well-developed foliation defined by alignment of mafic inclusions and schlieren, and down-dip lineation defined by the alignment of hornblende phenocrysts and elongation of mafic inclusions. These fabrics are inferred to have formed during pluton crystallization. A moderately- to well-developed, subsolidus mylonitic

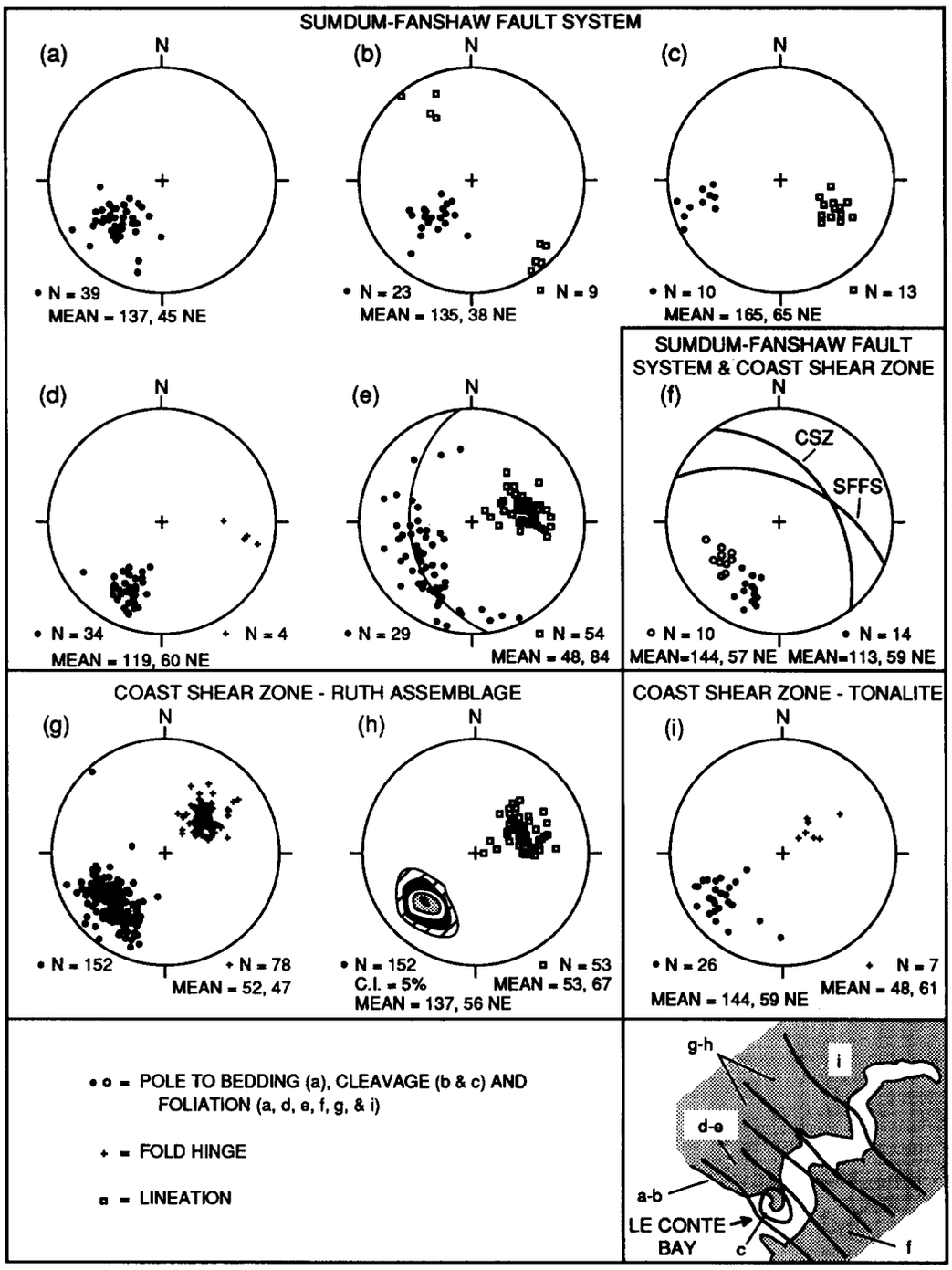

Fig. 12. Equal-area plots summarizing structural data from Le Conte Bay (Fig. 3). Inset map outlines stereonet domains. (a) Bedding and early-formed mid-Cretaceous foliation in Gravina strata north of Le Conte Bay. (b) Sumdum–Fanshaw fault system (SFFS) cleavage and fold hinges north of Le Conte Bay. (c) SFFS cleavage adjacent to the undeformed granodiorite at Indian Point. (d) SFFS foliation and mineral lineation in Le Conte Bay. (e) Early-formed foliation and SFFS fold hinges in Le Conte Bay. Poles to the foliation define a great circle with a pole of 44°, 86°. (f) SFFS and CSZ foliation pairs observed in outcrop. The difference in orientations is similar to that observed between SFFS and CSZ plots in (d) and (g). (g) Coast shear zone (CSZ) foliation and mineral stretching lineations in the Ruth assemblage. (h) Fold hinges and contoured plot of foliation plotted in (g). (i) CSZ foliation and mineral lineation in the tonalite in Le Conte Bay.

foliation, defined by alignment of biotite, quartz ribbons and fine-grained dynamically recrystallized quartz and biotite bands, is observed along the western pluton margins. The magmatic and solid-state fabrics are coplanar and colinear with one another as well as with the foliation and lineation in the subjacent Ruth assemblage (Figs. 11f and 12i).

Shear sense indicators in the Coast shear zone were commonly (1) not well developed due to extreme flattening and/or equigranular character of the rocks or (2) poorly preserved due to late- or post-kinematic recrystallization. In addition, the rocks possess indicators with conflicting senses of shear. Mesoscopic shear bands, asymmetric foliation boudinage, and occasional rotated porphyroclasts typically suggest east-side-up or reverse sense of shear. In contrast, west-side-up or normal

displacement is locally suggested by *c*-plane and shear band orientations, displacement sense across small shear zones, porphyroclast asymmetries, oblique foliation defined by dynamically recrystallized quartz aggregates, and folds in recrystallization tails. Rare *c*-plane orientations within the Paleocene tonalites suggest west-side-up displacement. Based on these kinematic observations, we conclude that the Coast shear zone records components of west-side-up as well as east-side-up displacement along the western flank of the Coast Mountains batholith.

Age constraints on the Coast shear zone

Primary intrusive relations between the Paleocene tonalites and Ruth assemblage are suggested by (1) the presence of small tonalitic sills intruding the Ruth assemblage and thin screens of the Ruth assemblage within the tonalite (Figs. 3 and 4) and (2) thermal metamorphism of the Ruth assemblage adjacent to the tonalite recorded by the appearance of sillimanite, coarse-grained calc-silicate assemblages in marbles, and secondary rims on garnets, none of which are observed west of the Coast shear zone (McClelland *et al.* 1991). Magmatic fabrics in the Paleocene tonalites are interpreted to reflect structurally controlled, syntectonic emplacement of the plutons within the Coast shear zone. Sub-solidus fabrics in the tonalites record post-emplacement deformation. We conclude from these observations that the Coast shear zone evolved prior to 63.5 ± 1 Ma and continued at least through 59.5 ± 1 Ma. The W-dipping dikes in Thomas Bay (Fig. 4) and on the Stikine River (Fig. 2) indicate that ductile deformation within the Coast shear zone ceased by approximately 50 Ma.

Eocene and younger deformation

In Thomas and Le Conte Bays, mid-Cretaceous and Paleocene shear zones are commonly cut by cm-thick brittle fault zones with normal displacement. Direction and sense of slip determined by striae, m-scale offsets and asymmetry of drag folds indicate reverse, normal and right-lateral strike-slip offset on NW- to NE-striking, E- and W-dipping fault sets. These brittle structures are most likely related to continued post-early Eocene uplift of the Coast Mountains batholith region similar to that observed in the southern Coast Mountains (Parrish 1983).

REGIONAL CORRELATION OF THE SUMDUM–FANSHAW FAULT SYSTEM

The Sumdum and Fanshaw faults have been traced from the Petersburg region to at least as far north as the Juneau region (Gehrels *et al.* 1990, in press). In southern Alaska, the Wrangellia terrane and Upper Jurassic–Lower Cretaceous strata of the Kahiltna terrane were underthrust beneath the southern margin of the Yukon–Tanana terrane in mid-Cretaceous time (Nokleberg *et al.* 1989, Stanley *et al.* 1990). West-vergent thrust faults in the Ketchikan region imbricate the Kah Shakes sequence (Yukon–Tanana terrane), Alava sequence (Taku terrane), Alexander terrane and Gravina belt (Rubin *et al.* 1990, Rubin and Saleeby in press). To the south, the Prince Rupert shear zone is inferred to mark the eastern margin of the Alexander terrane (Crawford *et al.* 1987). In both the Ketchikan and Prince Rupert regions, the geometric, temporal, and metamorphic character of mid-Cretaceous deformation is strikingly similar to that observed in the Petersburg region. Rubin *et al.* (1990) include the Prince Rupert shear zone in a mid-Cretaceous thrust belt extending from the Ketchikan region to the San Juan Islands, northwestern Washington. In addition, relations similar to those observed in southeastern Alaska have recently been described in the Harrison Lake region, east of the southern Coast Mountains (Journeay 1990). We conclude that the Sumdum–Fanshaw fault system lies within a thrust belt that evolved in mid-Cretaceous time along the inner margin of the Alexander, Wrangellia and Peninsular terranes from northwestern Washington to southern Alaska.

REGIONAL CORRELATION OF THE COAST SHEAR ZONE

Ductile fabrics of probable Paleocene age in the Tracy Arm–Endicott Arm region south of Juneau (Stowell & Hooper, 1990, Gehrels *et al.* in press) most likely represent the northern continuation of the Coast shear zone. At the head of Port Houghton, a broad zone of west-side-up structures that deform mid-Cretaceous structures (Gehrels *et al.* in press) may reflect local widening of the Coast shear zone.

Immediately west of the Coast Mountains batholith in the Ketchikan–Prince Rupert region, the Work Channel–East Behm Canal lineament is underlain by a 250-km-long shear zone (Crawford *et al.* 1987, 1989) that is similar in age and geometry to the Coast shear zone. Steeply dipping fabrics in this southern shear zone truncate moderately NE-dipping mid-Cretaceous fabrics and, similar to the Coast shear zone, record a complex kinematic history with components of both west-side-up (Crawford *et al.* 1989) and east-side-up (Crawford *et al.* 1987) displacement. Hence, the shear zone that defines the Work Channel–East Behm Canal lineament is most likely the southern extension of the Coast shear zone (M. L. Crawford personal communication 1989, Crawford & Crawford 1991).

DISCUSSION

The Sumdum fault and correlative faults to the north and south accommodated crustal-scale imbrication of the Alexander–Wrangellia and Yukon–Tanana terranes in mid-Cretaceous time. Early-formed foliation and

thrust faults in the Gravina belt record imbrication and thickening during early phases of contraction. Pronounced mid-Cretaceous crustal thickening was accompanied by relatively high pressure metamorphism (Crawford *et al.* 1987, Brew *et al.* 1989, Stowell 1989, McClelland *et al.* 1991) and emplacement of synorogenic epidote-bearing plutons at mid-crustal levels (Crawford *et al.* 1987, Zen 1988, Cook *et al.* 1991). The plutons are interpreted as products of E-directed subduction west of the Alexander–Wrangellia terrane (Armstrong 1988, Arth *et al.* 1988, Van der Heyden 1989, Barker & Arth 1990). Mid-Jurassic deformation involving the Alexander terrane is inferred to record its accretion to the North American margin (McClelland & Gehrels 1990, Saleeby & Rubin 1990). This view is supported by observations that (1) metaclastic rocks correlative with the Gravina belt depositionally overlie the Taku and Yukon–Tanana terranes in the Ketchikan region (Rubin & Saleeby 1991a) and (2) Late Jurassic and Early Cretaceous plutons were emplaced across the Wrangellia–Stikine terrane boundary in British Columbia (Armstrong 1988, Van der Heyden 1989). Hence, mid-Cretaceous deformation west of the Coast Mountains reflects 'intraplate' shortening and closure of the Gravina intra-arc basin rather than collision and termination of subduction inboard of the Alexander–Wrangellia terrane. East-directed underthrusting of the Alexander–Wrangellia terrane was broadly coeval with E-vergent thrusting within and west of the Stikine terrane (McGroder 1989, Rusmore & Woodsworth 1989, Evenchick 1991) and contractional deformation in the Omineca belt (Archibald *et al.* 1983). Mid-Cretaceous shortening was also coincident with a sharp increase in the convergence rate between the Farallon and North American plates at approximately 100 Ma (Engebretson *et al.* 1985). From these observations we conclude that mid-Cretaceous deformation was related to changes in relative plate motion rather than terrane accretion.

Mid-Cretaceous crustal thickening was followed by significant Late Cretaceous to mid-Eocene uplift of rocks within and west of the Coast Mountains batholith (e.g. Harrison *et al.* 1979, Hollister 1982, Crawford *et al.* 1987). Pressure estimates from mid-Cretaceous metamorphic rocks and garnet–epidote-bearing plutons combined with current crustal thickness (35–40 km) in southeastern Alaska (Barnes 1977) suggest that rocks west of the Coast shear zone have experienced approximately 25–30 km of uplift since mid-Cretaceous time (Crawford *et al.* 1987, Zen 1988). Tonalitic plutons and metamorphic rocks within the Coast shear zone record rapid uplift to shallow crustal levels during Paleocene and Early Eocene time (Hollister 1982, Wood *et al.* 1987, Stowell 1989, McClelland *et al.* 1991). East-side-up tilting of rocks west of the batholith may have accompanied this uplift (McClelland *et al.* 1991). A minimum uplift of 10 km prior to mid-Eocene time has also been suggested for rocks within the Coast Mountains batholith (Gehrels *et al.* 1984, Barker *et al.* 1986, Hollister & Crawford 1990 and references therein). The Coast shear zone most likely evolved in response to this Late Cretaceous to mid-Eocene uplift. Decoupling across the shear zone, perhaps enhanced by emplacement of tonalitic plutons (Hollister & Crawford 1986), may have allowed differential uplift, in terms of magnitude, timing and shear sense, of rocks within and west of the batholith.

Plate motion reconstructions suggest that dextral oblique convergence dominated the northwestern North American margin during Paleocene to mid-Eocene uplift of the Coast Mountains batholith (Engebretson *et al.* 1985). Late stage shear band fabrics indicating dextral shear in the Juneau region (Stowell & Hooper 1990) may reflect oblique convergence along the North American margin but the regional extent of these fabrics is uncertain since they have not yet been recognized within the Coast shear zone to the south. The dominance of subvertical dip-slip shear indicators suggests that the shear zone largely accommodated uplift rather than significant dextral translation.

CONCLUSIONS

Our structural and geochronologic studies in the Petersburg region indicate that the Gravina belt, Taku terrane and Yukon–Tanana equivalent Ruth assemblages were juxtaposed along the W-vergent Sumdum and Fanshaw faults during mid-Cretaceous time. The Sumdum–Fanshaw fault system and older fabrics in Albian strata of the Gravina belt record progressive deformation associated with the E-directed underthrusting of the Alexander–Wrangellia terrane beneath the Yukon–Tanana and Stikine terranes. Age data from syn- and post-tectonic plutons suggest that deformation was ongoing at 92.9 ± 3 Ma but deformation in the Gravina belt had generally ceased 90 Ma. The Sumdum–Fanshaw fault system is an integral part of a mid-Cretaceous thrust system that extends at least from southern Alaska to northern Washington and, over much of its length, places rocks of continental margin affinity over Upper Jurassic–Lower Cretaceous intra-arc basinal strata (Gehrels *et al.* 1990, Rubin *et al.* 1990). Mid-Cretaceous deformation in southeastern Alaska most likely records variations in relative plate motion and/or subduction parameters rather than terrane collision.

The Late Cretaceous–Early Tertiary Coast shear zone truncates and modifies the mid-Cretaceous thrust belt. This deformation preceded, controlled, and outlasted the emplacement of the tonalite plutons in the western Coast Mountains batholith. Kinematic relations in the Coast shear zone suggest a complex history of dip-slip displacement associated with uplift of rocks within and adjacent to the Coast Mountains batholith. We conclude that west-side-up (normal) displacement within this zone is significant. West-side-up displacement in the shear zone and east-side-up tilting of rocks west of the Coast Mountains batholith support the conclusion of Butler *et al.* (1989) that discordant paleomagnetic data from plutonic rocks west of and within the Coast Mountains batholith result from tilting rather than large-scale

translation. The Coast shear zone apparently accommodated the collapse of overthickened crust that developed during mid-Cretaceous compressional events. Early Tertiary uplift of the Coast Mountains batholith and adjacent rocks are inferred to mark the transition from a Late Cretaceous compressional to a Paleocene–Eocene tensional or transtensional regime, synchronous with the onset of major extension in the southern Omenica belt (e.g. Parrish *et al.* 1988).

Acknowledgements—This research has been funded by National Science Foundation grants EAR-8616473, EAR-8706749 and EAR-8903764 awarded to Gehrels and Patchett and research grants awarded to McClelland by the Geological Society of America, Sigma Xi, ARCO and University of Arizona. We thank D. A. Brew, M. L. Crawford, C. M. Rubin and J. B. Saleeby for useful discussions.

REFERENCES

Archibald, D. A., Glover, J. K., Price, R. A., Farrar, E. & Carmichael, D. M. 1983. Geochronology and tectonic implications of magmatism and metamorphism, southern Kootenay arc and neighboring regions, southeastern British Columbia—I. Jurassic to mid-Cretaceous. *Can. J. Earth Sci.* **20**, 1891–1913.

Armstrong, R. L. 1988. Mesozoic and early Cenozoic magmatic evolution of the Canadian Cordillera. In: *Processes in Continental Lithospheric Deformation* (edited by Clark, S. P., Jr., Burchfiel, B. C. & Suppe, J.). *Spec. Pap. geol. Soc. Am.* **218**, 55–91.

Arth, J. G., Barker, F. & Stern, T. W. 1988. Coast batholith and Taku plutons near Ketchikan, Alaska: petrography, geochronology, geochemistry, and isotopic character. *Am. J. Sci.* **288A**, 461–489.

Barker, F. & Arth, J. G. 1990. Two traverses across the Coast batholith, southeastern Alaska. In: *The Nature of Cordilleran Magmatism* (edited by Anderson, J. L.). *Spec. Pap. geol. Soc. Am.* **174**, 395–405.

Barker, F., Arth, J. G. & Stern, T. W. 1986. Evolution of the Coast batholith along the Skagway traverse, Alaska and British Columbia. *Am. Miner.* **71**, 632–643.

Barnes, D. F. 1977. Bouger gravity map of Alaska. *U.S. geol. Surv. Geophys. Investigations Map* GP-913, scale 1:2,500 000.

Berg, H. C., Jones, D. L. & Richter, D. H. 1972. Gravina–Nutzotin belt—significance of an upper Mesozoic sedimentary and volcanic sequence in southern and southeastern Alaska. *Prof. Pap. U.S. geol. Surv.* **800-D**, D1–D24.

Brew, D. A. & Ford, A. B. 1978. Megalineament in southeastern Alaska marks southwest edge of Coast Range batholithic complex. *Can. J. Earth Sci.* **15**, 1763–1772.

Brew, D. A. & Ford, A. B. 1981. The Coast plutonic complex sill, southeastern Alaksa. *U.S. geol. Surv. Circ.* **823-B**, B96–B98.

Brew, D. A., Ford, A. B. & Himmelberg, G. R. 1989. Evolution of the western part of the Coast plutonic-metamorphic complex, south-eastern Alaska, USA: a summary. In: *Evolution of Metamorphic Belts* (edited by Daly, J. S., Cliff, R. A. & Yardley, B. W. D.). *Spec. Publs geol. Soc. Lond.* **43**, 447–452.

Brew, D. A., Ovenshine, A. T., Karl, S. M. & Hunt, S. J. 1984. Preliminary reconnaissance geologic map of the Petersburg and parts of the Port Alexander and Sumdum quadrangles, southeastern Alaska. *U.S. geol. Surv. Open-file Rep.* **84-405**, scale 1:250 000.

Buddington, A. F. & Chapin, T. 1929, Geology and mineral deposits of southeastern Alaska. *Bull. U.S. geol. Surv.* **800**.

Butler, R. F., Gehrels, G. E., McClelland, W. C., May, S. R. & Klepacki, D. 1989. Discordant paleomagnetic poles from the Canadian Coast Plutonic Complex: regional tilt rather than large-scale displacement? *Geology* **17**, 691–694.

Coney, P. J. & Jones, D. L. 1985. Accretion tectonics and crustal structure in Alaska. *Tectonophysics* **119**, 265–283.

Cook, R. D., Crawford, M. L., Omar, G. I. & Crawford, W. A. 1991. Magmatism and deformation, southern Revillagigedo Island, southeastern Alaska. *Bull. geol. Soc. Am.* **103**, 829–841.

Crawford, M. L. & Crawford, W. A. 1991. Magma emplacement in a convergent tectonic orogen, southern Revillagigedo Island, southeastern Alaska. *Can. J. Earth Sci.* **28**, 929–938.

Crawford, M. L., Crawford, W. A. & Cook, R. D. 1989. Magmatism and tectonism, central Coastal Orogen, Alaska and British Columbia. *EOS* **70**, 1299.

Crawford, M. L., Hollister, L. S. & Woodsworth, G. J. 1987. Crustal deformation and regional metamorphism across a terrane boundary, Coast plutonic complex, British Columbia. *Tectonics* **6**, 343–361.

Douglass, S. L., Webster, J. H., Burrell, P. D., Lanphere, M. L. & Brew, D. A. 1989. Major element chemistry, radiometric values, and locations of samples from the Petersburg and parts of the Port Alexander and Sumdum quadrangles, southeastern Alaska. *U.S. geol. Surv. Open-file Rep.* **89-527**.

Engebretson, D. C., Cox, A. & Gordon, R. G. 1985. Relative motions between oceanic and continental plates in the Pacific basin. *Spec. Pap. geol. Soc. Am.* **206.**

Evenchick, C. A. 1991. Geometry, evolution, and tectonic framework of the Skeena fold belt, north-central British Columbia. *Tectonics* **10**, 527–546.

Gehrels, G. E. 1990. Late Proterozoic-Cambrian metamorphic basement of the Alexander terrane on Long and Dall Islands, SE Alaska. *Bull. geol. Soc. Am.* **102**, 760–767.

Gehrels, G. E. & Berg, H. C. 1984. Geologic map of southeastern Alaska. *U.S. geol. Surv. Open-file Rep.* **84-886**, scale 1:600 000.

Gehrels, G. E., Saleeby, J. S. & Brew, D. A. 1984. Progress report on U/Pb (zircon) geochronologic studies in the Coast plutonic–metamorphic complex east of Juneau, southeastern Alaska. *U.S. geol. Surv. Circ.* **939**, 100–102.

Gehrels, G. E., McClelland, W. C., Samson, S. D. & Patchett, P. J. 1991a. U–Pb geochronology of detrital zircons from a continental margin assemblage in the northern Coast Mountains, southeastern Alaska. *Can. J. Earth Sci.* **28**, 1285–1300.

Gehrels, G. E., McClelland, W. C., Samson, S. D., Patchett, P. J. & Brew, D. A. 1991b. U–Pb geochronology of Late Cretaceous and early Tertiary plutons in the northern Coast Mountains batholith. *Can. J. Earth Sci.* **28**, 899–911.

Gehrels, G. E., McClelland, W. C., Samson, S. D., Patchett, P. J. & Jackson, J. L. 1990. Ancient continental margin assemblage in the northern Coast Mountains, southeast Alaska and northwest Canada. *Geology* **18**, 208–211.

Gehrels, G. E., McClelland, W. C., Samson, S. D., Patchett, P. J. & Orchard, M. J. In press. Geologic and tectonic relations of the Gravina belt and the Taku and Yukon–Tanana terranes between Cape Fanshaw and Taku Inlet, southeastern Alaska. *Tectonics.*

Harrison, T. M., Armstrong, R. L., Naeser, C. W. & Harakal, J. E. 1979. Geochronology and thermal history of the Coast Plutonic Complex, near Prince Rupert, British Columbia. *Can. J. Earth Sci.* **16**, 400–410.

Hollister, L. S. 1982. Metamorphic evidence for rapid (2 mm/yr) uplift of a portion of the central gneiss complex, Coast Mountains, B. C. *Can. Mineralogist* **20**, 319–332.

Hollister, L. S. & Crawford, M. L. 1986. Melt enhanced deformation: a major tectonic process. *Geology* **14**, 558–561.

Hollister, L. S. & Crawford, M. L. 1990. Crustal formation at depth during continental collision. In: *Exposed Cross-sections of the Continental Crust* (edited by Salisbury, M. H. & Fountain, D. M.). Kluwer, Norwell, Massachusetts, 215–226.

Jones, D. L., Irwin, W. P. & Ovenshine, A. T. 1972. Southeastern Alaska—a displaced continental fragment. *Prof. Pap. U.S. geol. Surv.* **800-B**, B211–B217.

Jones, D. L., Silberling, N. J. & Hillhouse, J. 1977. Wrangellia—a displaced terrane in northwestern North America. *Can. J. Earth Sci.* **14**, 2565–2577.

Journeay, J. M. 1990. A progress report on the structural and tectonic framework of the southern Coast belt, British Columbia. *Geol. Surv. Pap. Can.* **90-1E**, 183–195.

McClelland, W. C. & Gehrels, G. E. 1990. Geology of the Duncan Canal shear zone: evidence for Early–Middle Jurassic deformation of the Alexander terrane, southeastern Alaska. *Bull. geol. Soc. Am.* **102**, 1378–1392.

McClelland, W. C., Anovitz, L. M. & Gehrels, G. E. 1991. Thermobarometric constraints on the structural evolution of the Coast Mountains batholith, central southeastern Alaska. *Can. J. Earth Sci.* **28**, 912–928.

McClelland, W. C., Gehrels, G. E., Samson, S. D. & Patchett, P. J. 1992. Protolith relations of the Gravina belt and Yukon–Tanana terrane in central southeastern Alaska. *J. Geol.* **100**, 107–123.

McGroder, M. F. 1989. Structural geometry and structural evolution of the eastern Cascades foldbelt, Washington and British Columbia. *Can. J. Earth Sci.* **26**, 1586–1602.

Monger, J. W. H. & Berg, H. C. 1987. Lithotectonic terrane map of

western Canada and southeastern Alaska. *U.S. geol. Surv. Misc. Field Studies Map* **1874-B**, scale 1:2,500 000.

Monger, J. W. H., Price, R. A. & Tempelman-Kluit, D. J. 1982. Tectonic accretion and the origin of the two major metamorphic welts in the Canadian Cordillera. *Geology* **10**, 70–75.

Mortensen, J. K. In press. Pre-mid-Mesozoic tectonic evolution of the Yukon–Tanana terrane, Yukon and Alaska. *Tectonics*.

Nokleberg, W. J., Foster, H. L. & Aleinikoff, J. N. 1989. Geology of the northern Copper River basin, eastern Alaska Range, and southern Yukon–Tanana upland. In: *Alaskan Geological and Geophysical Transect Valdez to Coldfoot, Alaska* (edited by Nokleberg, W. J. & Fisher, M. A.). *Am. Geophys. Un. Field Trip Guidebook* **T104**, 34–63.

Palmer, A. R. 1983. The decade of North American geology time scale. *Geology* **11**, 503–504.

Parrish, R. R. 1983. Cenozoic thermal evolution and tectonics of the Coast Mountains of British Columbia 1. fission track dating, apparent uplift rates, and patterns of uplift. *Tectonics* **2**, 601–631.

Parrish, R. R., Carr, S. D. & Parkinson, D. L. 1988. Eocene extensional tectonics and geochronology of the southern Omenica belt, British Columbia and Washington. *Tectonics* **7**, 181–212.

Rubin, C. M. & Saleeby, J. B. 1991a. Tectonic framework of the upper Paleozoic and lower Mesozoic Alava sequence: A revised view of the polygenetic Taku terrane in southern Alaska. *Can. J. Earth Sci.* **28**, 881–893.

Rubin, C. M. & Saleeby, J. B. 1991b. The Gravina sequence—remnants of a mid-Mesozoic oceanic arc complex in southern southeast Alaska. *J. geophys. Res.* **96**, 14,551–14,568.

Rubin, C. M. & Saleeby, J. B. In press. Thrust tectonics and Cretaceous intracontinental shortening in southeast Alaska. In: *Thrust Tectonics* (edited by McClay, K.). Unwin Hyman, London.

Rubin, C. M., Saleeby, J. B., Cowan, D. S., Brandon, M. T. & McGroder, M. F. 1990. Regionally extensive mid-Cretaceous west-vergent thrust system in the northwestern Cordillera: Implications for continental margin tectonism. *Geology* **18**, 276–280.

Rusmore, M. E. & Woodsworth, G. J. 1989. A note on the Coast–Intermontane belt transition, Mount Waddington map area. *Geol. Surv. Pap. Can.* **89-1E**, 163–167.

Saleeby, J. B. & Rubin, C. M. 1990. Tectonic intercalation of crystalline nappes and basinal overlap relations in southern SE Alaska: implications for initial stages of Insular superterrane accretion. *EOS* **71**, 1591.

Samson, S. D., Patchett, P. J., McClelland, W. C. & Gehrels, G. E. 1991. Nd isotopic characterization of the metamorphic rocks in the Coast mountains, Alaskan and Canadian Cordillera: ancient crust bounded by juvenile terranes. *Tectonics* **10**, 770–780.

Stacey, J. S. & Kramers, J. D. 1975. Approximation of terrestrial lead isotope evolution by a two-stage model. *Earth Planet. Sci. Lett.* **26**, 207–221.

Stanley, W. D., Labson, V. F., Nokleberg, W. J., Csejtey, B., Jr. & Fisher, M. A. 1990. The Denali fault system and Alaska Range of Alaska: Evidence for underplated Mesozoic flysch from magnetotelluric surveys. *Bull. geol. Soc. Am.* **102**, 160–173.

Stowell, H. H. 1989. Silicate and sulphide thermobarometry of low- to medium-grade metamorphic rocks from Holkham Bay, south-east Alaska. *J. metamorph. Geol.* **7**, 343–358.

Stowell, H. H. & Hooper, R. J. 1990. Structural development of the western metamorphic belt adjacent to the Coast Plutonic Complex, southeastern Alaska: evidence from Holkham Bay. *Tectonics* **9**, 391–407.

Tobisch, O. T. & Patterson, S. R. 1988. Analysis and interpretation of composite foliations in areas of progressive deformation. *J. Struct. Geol.* **10**, 745–754.

Twenhofel, W. S. & Sainsbury, C. L. 1958. Fault patterns in southeastern Alaska. *Bull. geol. Soc. Am.* **69**, 1431–1442.

Van der Heyden, P. 1989. U–Pb and K–Ar geochronometry of the Coast Plutonic Complex, 53°N to 54°N, British Columbia, and implications for the Insular–Intermontane superterrane boundary. Unpublished Ph.D. thesis, University of British Columbia, Vancouver.

Wheeler, J. O. & McFeely, P. 1987. Tectonic assemblage map of the Canadian Cordillera. *Geol. Surv. Can. Open-file Rep.* **1565**, scale 1:2,000,000.

Wood, D. J., Stowell, H. H. & Onstott, T. C. 1987. Uplift and cooling rates from thermochronology ($^{40}Ar/^{39}Ar$) of the Coast Plutonic Complex sill, SE Alaska. *Geol. Soc. Am. Abs. w. Prog.* **19**, 896.

Zen, E. 1988. Tectonic significance of high-pressure plutonic rocks in the western Cordillera of North America. In: *Metamorphism and Crustal Evolution of the Western United States* (edited by Ernst, W. G.). Prentice-Hall, Englewood Cliffs, New Jersey, 42–67.